Instanton-based Kramers turnover theory

Eli Pollak
Chemical and Biological Physics Department, Weizmann Institute of Science, 76100 Rehovoth, Israel

(Received 9 November 2023; accepted 5 February 2024; published 26 February 2024)

The quantum version of Kramers turnover theory is generalized beyond the parabolic barrier approximation. The result is a uniform instanton-based quantum Kramers turnover theory that does not display any divergence at what is known as the crossover temperature. The theory is analyzed using a model of a particle trapped in a cubic potential. As the temperature is lowered, the maximum in the Kramers turnover curve moves to lower friction values. When the temperature is sufficiently low, the quantum rate at low friction becomes almost independent of the friction strength.

DOI: 10.1103/PhysRevA.109.022242

I. INTRODUCTION

Originally, the central challenge underlying what is known as "Kramers' turnover theory" was to find an expression for the thermal rate of escape of a trapped classical particle as a function of the friction acting on it, for all values of the friction. Kramers [1], using a Langevin equation model, showed that at low friction the rate increases linearly with the friction coefficient, while at high friction it decreases inversely to the friction. The challenge was to find a solution which covers the whole range of friction coefficients. This challenge was answered in two steps. The first step was by Mel'nikov and Meshkov (MM) [2], who solved for the energy activation and deactivation when the friction was small to moderate. The second was to merge the MM formal derivation within a normal-mode picture of the dynamics [3], leading to an expression valid for all values of the friction coefficient [4]. This last result, known as Pollak-Grabert-Hänggi (PGH) theory [5], was recently extended to include also the rate of escape and diffusion of a particle on a periodic surface [6,7]. Kramers' turnover was observed experimentally [8]. A recent review of the theory may be found in Ref. [9].

The turnover theory was generalized to include quantum tunneling effects in Ref. [10] and followed by similar developments in Refs. [5,11]. The quantum version of the turnover theory was based on the usage of parabolic barrier transmission and reflection coefficients. As a result, it was valid only for temperatures higher than the "crossover temperature" $k_BT \geqslant \frac{\hbar\lambda^\ddagger}{2\pi}$, where $\lambda^\ddagger$ is the normal-mode barrier frequency as described below. This difficulty was not limited to Kramers' theory. Wolynes [12] derived an expression for the rate in the spatial-diffusion-limited regime which suffered from the same difficulty. Miller [13] and later Coleman [14] derived what is known as the instanton (also known as the bounce in the physics literature [15,16]) expression for the thermal rate, and it, too, diverged when the temperature reached the "crossover temperature." Over the years different approaches were suggested to overcome this difficulty [17–23]. This divergence problem was resolved recently in Refs. [24,25] by employing Kemble's version [26] of the semiclassical transmission and reflection probabilities leading to a uniform instanton rate theory [Eq. (3.7) below]. If one defines the crossover temperature as that temperature at which the instanton energy equals the barrier energy, then in the uniform instanton rate theory this occurs when $\hbar\beta\lambda^\ddagger = \pi$ [$\lambda^\ddagger$ is the friction-dependent barrier frequency, see Eq. (2.5) below] but not 2π, as in the old theory. The crossover temperature in the uniform semiclassical theory is twice as high as the "old" crossover temperature. Not less important is the fact that there does not exist a divergence at the "crossover temperature" as in the old theory. The purpose of the present paper is to use the uniform instanton rate theory to generalize the quantum turnover theory so that it, too, does not suffer from divergences. This instanton-based turnover theory turns out to be a generalization of the quantum turnover formula of Ref. [10].

In Sec. II we review briefly the latest version of turnover theory [6,27] based on the parabolic barrier reflection and transmission coefficients. We then present in Sec. III the uniform semiclassical version of Wolynes' tunneling correction factor as derived in Ref. [25]. This gives a spatial diffusion factor which does not diverge at the "crossover temperature." The central part of this paper is the derivation of the uniform instanton-based depopulation factor, leading to a divergenceless quantum turnover theory expression for the rate. To get a feeling for the resulting uniform instanton turnover theory, we present some numerical applications using a cubic-potential-based model for the escape rate of a particle trapped in a well. We end with a Discussion of the assumptions underlying the theory and their limitations.

II. SHORT REVIEW OF TURNOVER THEORY

The goal of the turnover theory is to provide an expression for the escape rate of a particle with mass M and coordinate q trapped in a well, located at q_0 with harmonic frequency ω_0 and energy $E = 0$, which can escape through a barrier located at $q = 0$ with imaginary barrier frequency $\omega^\ddagger$ and barrier energy $V^\ddagger$ which separates the well from a continuum. The classical equation of motion of the particle is a generalized Langevin equation (GLE) of the form

$$M\ddot{q} + \frac{dV(q)}{dq} + M\int_0^t dt'\gamma(t-t')\dot{q}(t') = F(t). \qquad (2.1)$$

$F(t)$ is a Gaussian random force with zero mean and correlation function,

$$\langle F(t)F(t')\rangle = Mk_BT\gamma(t-t'), \tag{2.2}$$

where $\gamma(t)$ is the friction function, k_B is Boltzmann's constant, and T is the temperature. The potential is written as

$$V(q) = -\tfrac{1}{2}M\omega^{\ddagger 2}q^2 + V_1(q), \tag{2.3}$$

and $V_1(q)$ is termed the nonlinear part of the potential function. Kramers' turnover theory is aimed at providing an expression for the thermal escape rate of the particle as a function of friction strength, friction memory, and temperature.

When one ignores the nonlinear part of the potential, the resulting Hamiltonian has a quadratic form and may be diagonalized [28]. The (unstable) mass-weighted normal mode and associated momentum are denoted as ρ and p_ρ, respectively. The stable bath normal-mode coordinates and momenta are denoted as y_j and p_{y_j}, respectively. The full Hamiltonian may then be expressed as

$$H = \frac{p_\rho^2}{2} - \frac{1}{2}\lambda^{\ddagger 2}\rho^2 + V_1(q) + \frac{1}{2}\sum_{j=1}^{N}\left[p_{y_j}^2 + \lambda_j^{\ddagger 2}y_j^2\right], \tag{2.4}$$

where $\lambda_j^\ddagger$ denotes the frequency of the jth normal mode at the barrier. $\lambda^\ddagger$ denotes the unstable normal-mode barrier frequency, and it may be obtained through the Kramers-Grote-Hynes relation [1,29], formalized by Hänggi and Mojtabai [30]:

$$\lambda^{\ddagger 2} + \hat{\gamma}(\lambda^\ddagger)\lambda^\ddagger = \omega^{\ddagger 2}, \tag{2.5}$$

where the "hat" notation as in $\hat{\gamma}(s)$ denotes the Laplace transform, in this case, of the time-dependent friction. The system coordinate q may be expressed in terms of the normal modes as

$$\sqrt{M}q = u_{00}\rho + u_1\sigma, \tag{2.6}$$

with

$$u_1\sigma = \sum_{j=1}^{N} u_{j0}y_j \tag{2.7}$$

and

$$u_1^2 = 1 - u_{00}^2 = \sum_{j=1}^{N} u_{j0}^2. \tag{2.8}$$

The nonlinear part of the potential $V_1(q)$ couples the motion of the unstable normal mode to that of the stable normal modes. The matrix element u_{j0} is the projection of the system coordinate on the jth normal mode. The projection of the system coordinate on the unstable mode u_{00} is given by the relation [4,28]

$$u_{00}^2 = \left[1 + \frac{1}{2}\left(\frac{\hat{\gamma}(\lambda^\ddagger)}{\lambda^\ddagger} + \left.\frac{\partial\hat{\gamma}(s)}{\partial s}\right|_{s=\lambda^\ddagger}\right)\right]^{-1}. \tag{2.9}$$

The normal-mode "friction kernel" is defined as

$$K(t-t') = \sum_{j=1}^{N}\frac{u_{j0}^2}{\lambda_j^{\ddagger 2}}\cos[\lambda_j^\ddagger(t-t')]. \tag{2.10}$$

Using properties of the normal-mode transformation (see, for example, Eq. (2.17) of Ref. [28]) one may readily express the Laplace transform of the kernel in terms of the Laplace transform of the friction function so that it is known in the continuum limit. The spectral density of the stable modes is [10,28]

$$I(\lambda) = \lambda\mathrm{Re}[\hat{\mathrm{K}}(\mathrm{i}\lambda)] = \frac{\lambda\mathrm{Re}[\hat{\gamma}(\mathrm{i}\lambda)]}{\left(\omega^{\ddagger 2}+\lambda^2\right)^2 + \lambda^2\hat{\gamma}(\mathrm{i}\lambda)\hat{\gamma}(-\mathrm{i}\lambda)}. \tag{2.11}$$

To obtain the turnover expression for the rate, we use the modern version of the turnover theory, as described in Refs. [6,27]. The zeroth-order dynamics of the unstable normal mode is determined by the zeroth-order unstable mode Hamiltonian:

$$\begin{aligned} H_\rho &= \frac{p_\rho^2}{2} + V\left(\frac{\lambda^\ddagger}{\sqrt{M}\omega^\ddagger}\rho\right) \\ &= \frac{p_\rho^2}{2} - \frac{1}{2}\lambda^{\ddagger 2}\rho^2 + V_1\left(\frac{\lambda^\ddagger}{\sqrt{M}\omega^\ddagger}\rho\right). \end{aligned} \tag{2.12}$$

Close to the barrier top, the zeroth-order barrier remains quadratic in the unstable mode coordinate. The zeroth-order dynamics of the stable bath normal modes is that of a collection of uncoupled harmonic oscillators.

Expanding the Hamiltonian to leading order in the coupling to the bath, one obtains a forced oscillator equation of motion for the stable modes, where the force is determined by the zeroth-order motion of the unstable mode. Following the PGH methodology, the (reduced) average energy $\delta(E) = \beta\Delta E(E)$ (with $\beta = 1/(k_BT)$ the inverse temperature) gained by the bath as the unstable mode traverses from the barrier over the well and back to the barrier at the energy E as given by

$$\begin{aligned} \delta(E) \equiv \frac{\beta}{2\pi M}\int_{-\infty}^{\infty} d\lambda\lambda I(\lambda) \\ \times \left|\int_{-\tau(E)/2}^{\tau(E)/2} dt\,\exp(-i\lambda t)V_1'\left(\frac{\lambda^\ddagger\rho_{t,0}}{\sqrt{M}\omega^\ddagger}\right)\right|^2, \end{aligned} \tag{2.13}$$

where it is understood that $\rho_{t,0}$ is the unperturbed periodic classical trajectory of the unstable mode initiated at energy E at the turning point close to the barrier, moving over the well to the other turning point and returning. The period of the orbit is $\tau(E)$. Quantum effects may be added following the same developments as in Ref. [10], and finite barrier effects which are important when $\beta V^\ddagger \sim 1$ may be included as in Ref. [6]. To simplify, these will be henceforth ignored.

The expression for the quantum thermal rate as derived in Ref. [10] is a product of three factors:

$$\Gamma(\beta) = \frac{\omega_0}{2\pi}\exp(-\beta V^\ddagger)\Upsilon\frac{\lambda^\ddagger}{\omega^\ddagger}\Xi. \tag{2.14}$$

$\frac{\omega_0}{2\pi}\exp(-\beta V^\ddagger)$ is the harmonic classical transition-state theory rate, Υ is termed the depopulation factor and accounts for the energetic excitation and deexcitation of the particle in the well, and $\frac{\lambda^\ddagger}{\omega^\ddagger}\Xi_W$ is the spatial diffusion factor. In the previous quantum theory of Ref. [10], the spatial diffusion factor as well as the depopulation factor were derived by

assuming a parabolic barrier approximation for the energy-dependent transmission and reflection probability through the barrier. As a result, the spatial diffusion factor was taken to be the transition-state theory expression for the parabolic barrier [31]:

$$\Xi_W = \frac{\omega^\ddagger}{\omega_0}\frac{\sinh\left(\frac{\hbar\beta\lambda_0}{2}\right)}{\sin\left(\frac{\hbar\beta\lambda^\ddagger}{2}\right)}\pi_{j=1}^N\left[\frac{\sinh\left(\frac{\hbar\beta\lambda_j}{2}\right)}{\sinh\left(\frac{\hbar\beta\lambda_j^\ddagger}{2}\right)}\right]. \tag{2.15}$$

Here, the potential $V(q)$ is assumed to be harmonic around the well so that the Hamiltonian in the region of the well is quadratic and may also be diagonalized to give the $N+1$ stable frequencies λ_j, $j=0,\ldots,N$. As shown in Ref. [31], Eq. (2.15) is equivalent to Wolynes's expression

$$\Xi_W = \pi_{k=1}^\infty \frac{\left[\omega_0^2+\nu_k^2+\nu_k\hat{\gamma}(\nu_k)\right]}{\left[-\omega^{\ddagger 2}+\nu_k^2+\nu_k\hat{\gamma}(\nu_k)\right]}, \tag{2.16}$$

where $\nu_k = \frac{2\pi k}{\hbar\beta}$ is the kth Matsubara frequency.

The turnover theory, like any quantum tunneling probability based on a parabolic barrier approximation, diverges when the inverse temperature is such that $\hbar\beta\lambda^\ddagger = 2\pi$. The depopulation factor as derived in Ref. [10] is also based on the parabolic barrier reflection and transmission probabilities so that it, too, is valid, provided that $\hbar\beta\lambda^\ddagger < 2\pi$. The central goal of this paper is to extend the quantum turnover theory such that it does not have a divergence.

III. UNIFORM INSTANTON SEMICLASSICAL RATE THEORY IN THE SPATIAL DIFFUSION LIMIT

To generalize the turnover theory it is necessary to derive the expression in the spatial-diffusion-limited regime so that it does not diverge, as well as to modify the derivation of the depopulation factor so that it includes anharmonic effects in the tunneling probabilities. For the sake of completeness, we briefly review here the uniform instanton spatial-diffusion-limited rate as presented in Ref. [24]. Throughout, we assume that the motion along the unstable mode is separable from the other modes, governed by the Hamiltonian of Eq. (2.12). The quantum transmission probability is then approximated using the uniform expression of Kemble [26], which involves a classical periodic orbit on the upside-down potential energy surface (the instanton) and is obtained with the classical Euclidean action. The assumption that this orbit may be obtained using the separable approximation is valid at high temperatures where the dynamics is determined mainly around the barrier energy. The assumption of separability becomes more questionable as the temperature is lowered and the motion occurs further away from the barrier top. There are additional limitations. In principle, in the well, especially at low energies, if the friction is not too large, one will have broadened resonance states, and these, too, should be taken into consideration. These limitations will be discussed below.

Using quantum transition-state theory, which is exact within the separable approximation we are using, one has that the rate expression is the ratio of the partition function of the stable modes at the barrier to the partition function of the reactants multiplied by the one-dimensional quantum thermal transmission factor through the barrier $\kappa(\beta)$:

$$\Gamma_{SD} = \frac{1}{2\pi\hbar\beta}\frac{Q^\ddagger}{Q_0}\kappa(\beta). \tag{3.1}$$

The reactant is in the well and assumed to be harmonic so that

$$Q_0 = \pi_{j=0}^N\left[\frac{1}{2\sinh\left(\frac{\hbar\beta\lambda_j}{2}\right)}\right]. \tag{3.2}$$

The partition function of the stable normal modes at the barrier is

$$Q^\ddagger = \pi_{j=1}^N\left[\frac{1}{2\sinh\left(\frac{\hbar\beta\lambda_j^\ddagger}{2}\right)}\right]. \tag{3.3}$$

The transmission factor through the barrier is

$$\kappa(\beta) = \beta\int_0^\infty dE\,\exp(-\beta E)T(E), \tag{3.4}$$

where $T(E)$ is the transmission probability through the barrier at energy E. In the turnover theory of Ref. [10] this transmission factor was taken to be the parabolic barrier transmission factor

$$T_{pb}(E) = \frac{1}{1+\exp\left[\frac{2\pi}{\hbar\lambda^\ddagger}(V^\ddagger - E)\right]}, \tag{3.5}$$

and the reflection coefficient $R_{pb}(E) = 1 - T_{pb}(E)$. The corresponding parabolic barrier thermal transmission factor is well known,

$$\begin{aligned}\kappa_{pb}(\beta) &= \beta\int_{-\infty}^\infty dE\,\exp(-\beta E)T_{pb}(E)\\ &= \exp(-\beta V^\ddagger)\frac{\frac{\hbar\beta\lambda^\ddagger}{2}}{\sin\left(\frac{\hbar\beta\lambda^\ddagger}{2}\right)},\end{aligned} \tag{3.6}$$

and it diverges when $\hbar\beta\lambda^\ddagger = 2\pi$.

It is here that we first depart from the parabolic barrier approximation by assuming that the transmission and reflection probabilities at energy E are given by the uniform semiclassical expression of Kemble [26]:

$$T_{usc}(E) = \frac{1}{1+\exp\left[\frac{1}{\hbar}S(E)\right]} \equiv 1 - R_{usc}(E), \tag{3.7}$$

where $S(E)$ is usually taken to be the Euclidean action of the unstable mode through the barrier [13],

$$S(E) = \oint d\rho\sqrt{2\left[V\left(\frac{\lambda^\ddagger}{\sqrt{M}\omega^\ddagger}\rho\right) - E\right]}. \tag{3.8}$$

The thermal transmission factor may then be estimated by steepest descent, where the steepest descent condition at the (inverse) temperature β is such that the energy E_β of the instanton (the periodic orbit on the upside-down potential) is determined by

$$\begin{aligned}\hbar\beta &= -\frac{1}{1+\exp\left(-\frac{S(E_\beta)}{\hbar}\right)}\frac{dS(E_\beta)}{dE_\beta}\\ &= \frac{1}{1+\exp\left(-\frac{S(E_\beta)}{\hbar}\right)}\tau(E_\beta),\end{aligned} \tag{3.9}$$

where $\tau(E_\beta) = -\frac{dS(E_\beta)}{dE_\beta}$ is the period of the instanton at the energy E_β. Modifying the steepest descent estimate so that at high energies where the transmission coefficient goes to unity the integrand is exponential in the energy rather than Gaussian, as described in Ref. [24], one obtains the steepest descent estimate for the transmission factor

$$\kappa_{usc}(\beta) \simeq \exp\left[-\frac{\Phi(E_\beta)}{\hbar}\right] \times \sqrt{\frac{\pi\hbar\beta^2}{2\Phi_2(E_\beta)}}\left[1+\mathrm{erf}\left(\sqrt{\frac{\hbar\beta^2}{2\Phi_2(\mathrm{E}_\beta)}}\right)\right] + \exp\left[-\frac{\hbar\beta^2}{2\Phi_2(E_\beta)}\right], \tag{3.10}$$

where

$$\frac{\Phi(E)}{\hbar} = \beta E + \ln\left[1+\exp\left(-\frac{S(E)}{\hbar}\right)\right], \tag{3.11}$$

and $\Phi_2(E_\beta)$ is the second derivative with respect to the energy at the steepest descent energy $E = E_\beta$.

The spatial-diffusion-limited rate is thus

$$\Gamma_{SD} = \frac{1}{\pi\hbar\beta}\kappa_{usc}(\beta)\sinh\left(\frac{\hbar\beta\lambda_0}{2}\right)\pi_{j=1}^{N}\left[\frac{\sinh\left(\frac{\hbar\beta\lambda_j}{2}\right)}{\sinh\left(\frac{\hbar\beta\lambda_j^\ddagger}{2}\right)}\right] \equiv \frac{\omega_0}{2\pi}\exp(-\beta V^\ddagger)\frac{\lambda^\ddagger}{\omega^\ddagger}\Xi_{\mathrm{Uniform}}, \tag{3.12}$$

identifying the uniform semiclassical version of the Wolynes factor Ξ_W as

$$\Xi_{\mathrm{Uniform}} = \frac{\kappa_{usc}(\beta)}{\kappa_{pb}(\beta)}\Xi_W = \exp(\beta V^\ddagger)\kappa_{usc}(\beta)\pi_{k=1}^{\infty} \times \frac{\left[\omega_0^2+\nu_k^2+\nu_k\hat{\gamma}(\nu_k)\right](\nu_k+\lambda^\ddagger)}{\nu_k^2[\nu_k+\lambda^\ddagger+\hat{\gamma}(\nu_k)]}, \tag{3.13}$$

where the second line has been derived in Ref. [25]. It remains to derive an expression for the depopulation factor which is based on the uniform instanton approximation.

IV. THE DEPOPULATION FACTOR

To derive the expression for the depopulation factor, we follow as much as possible, using the same notation, the steps described in the Appendix of Ref. [10]. For this purpose we define the dimensionless energy

$$\varepsilon = \beta(E - V^\ddagger), \tag{4.1}$$

which vanishes at the barrier energy. We denote by $n(\varepsilon)$ the stationary probability for finding the system at (reduced) energy ε at the turning point closest to the barrier. At steady state (Eq. (4.3) of Ref. [10]),

$$n(\varepsilon) = \int_{-\infty}^{\infty} d\varepsilon' P(\varepsilon-\varepsilon')R_{usc}(\varepsilon')n(\varepsilon'), \tag{4.2}$$

where $P(\varepsilon-\varepsilon')$ is the transition probability kernel for the particle to start at the turning point next to the barrier with energy ε', move to the other turning point, and return to the barrier with energy ε. The details of this kernel are discussed further below. The lower bound of $-\infty$ in the equation is taken due to the fact that at $E = 0$, $\varepsilon = -\beta V^\ddagger$, and we assume that $\infty \simeq \beta V^\ddagger \gg 1$. The boundary condition on $n(\varepsilon)$ is that at sufficiently low energy it is the equilibrium probability as in Eq. (A6). In contrast to the choice of the parabolic barrier reflection and transmission coefficient used in Ref. [10], we introduce here the uniform semiclassical coefficients as in Eq. (3.7). Using the notation

$$N(\varepsilon) = R_{usc}(\varepsilon)n(\varepsilon), \tag{4.3}$$

one rewrites the steady-state equation as

$$\left(1+\exp\left[-\frac{1}{\hbar}S(\varepsilon)\right]\right)N(\varepsilon) = \int_{-\infty}^{\infty} d\varepsilon' P(\varepsilon-\varepsilon')N(\varepsilon'). \tag{4.4}$$

At this point we depart from the derivation of Ref. [10]. We are interested in the stationary probability at the instanton energy ε_β rather than at the barrier top. For this purpose we expand the action about the steepest descent energy up to the linear term:

$$S(\varepsilon) \simeq S(\varepsilon_\beta) - \frac{\tau(\varepsilon_\beta)}{\beta}(\varepsilon-\varepsilon_\beta). \tag{4.5}$$

Denoting the two-sided Laplace transform as

$$\tilde{N}(is) = \int_{-\infty}^{\infty} d\varepsilon N(\varepsilon)\exp(-\varepsilon s) \tag{4.6}$$

and taking the two-sided Laplace transform of the steady-state equation (4.4), one finds after rearranging that

$$\tilde{N}\left[i\left(s-\frac{\tau(\varepsilon_\beta)}{\hbar\beta}\right)\right] = -\exp\left[\frac{1}{\hbar}S(\varepsilon_\beta)+\frac{\tau(\varepsilon_\beta)\varepsilon_\beta}{\hbar\beta}\right][1-\tilde{P}(is)]\tilde{N}(is). \tag{4.7}$$

This result is identical in form to Eq. (A3) of the Appendix of Ref. [10], except for the additional constant term (not dependent on s) $\exp[\frac{1}{\hbar}S(\varepsilon_\beta)+\frac{\tau(\varepsilon_\beta)\varepsilon_\beta}{\hbar\beta}]$. As shown in the Appendix, one may then follow the derivation given in the Appendix of Ref. [10] to find the central result for the "uniform" depopulation factor:

$$\Upsilon_{\mathrm{uniform}} = \exp\left\{\frac{\hbar\beta}{\tau(E_\beta)}\sin\left(\frac{\pi\hbar\beta}{\tau(E_\beta)}\right)\int_{-\infty}^{\infty} dy \frac{\ln\left[1-\tilde{P}\left(y-\frac{i}{2}\right)\right]}{\left(\cosh\left[\frac{2\pi\hbar\beta}{\tau(E_\beta)}y\right]-\cos\left[\frac{\pi\hbar\beta}{\tau(E_\beta)}\right]\right)}\right\}. \tag{4.8}$$

This should be compared to the previous, parabolic barrier transmission probability–based result given in Eq. (4.13) of Ref. [10]:

$$\Upsilon_{pb} = \exp\left\{\frac{\hbar\beta\lambda^{\ddagger}}{2\pi}\sin\left(\frac{\hbar\beta\lambda^{\ddagger}}{2}\right)\int_{-\infty}^{\infty} dy \frac{\ln\left[1-\tilde{P}\left(y-\frac{i}{2}\right)\right]}{\left(\cosh\left[\hbar\beta\lambda^{\ddagger}y\right]-\cos\left[\frac{\hbar\beta\lambda^{\ddagger}}{2}\right]\right)}\right\}. \tag{4.9}$$

At high temperature, the energy of the instanton is close to the barrier so that $\tau(E_\beta) \simeq 2\pi/\lambda^{\ddagger}$ and the uniform result of Eq. (4.8) reduces formally to the result of Eq. (4.9). On the other hand, as may be seen from the steepest descent condition of Eq. (3.9), $\frac{\hbar\beta}{\tau(E_\beta)} \leqslant 1$, so that for any temperature $\sin(\frac{\pi\hbar\beta}{\tau(E_\beta)}) \geqslant 0$, and the so-called crossover temperature does not affect the uniform depopulation factor.

The final working expression for the rate is the turnover expression

$$\Gamma = \frac{\omega_0}{2\pi}\exp(-\beta V^{\ddagger})\frac{\lambda^{\ddagger}}{\omega^{\ddagger}}\Xi_{\text{Uniform}}\Upsilon_{\text{uniform}}, \tag{4.10}$$

and all divergences have been eliminated.

The remaining question is the kernel $\tilde{P}(y-\frac{i}{2})$. Ignoring the lowest-order quantum correction as in Eq. (3.23) of Ref. [10], we have that

$$\tilde{P}\left(y-\frac{i}{2}\right) = \exp\left[-\delta\left(E_\beta\right)\left(y^2+\frac{1}{4}\right)\right]. \tag{4.11}$$

In the parabolic-barrier-based turnover theory, the energy loss is associated with the orbit that is initiated asymptotically close to the barrier top, crosses the well, reaches the inner turning point, and then comes back to the barrier. In the present uniform instanton-based theory, the energy loss is along the trajectory whose energy is the steepest descent instanton energy E_β rather than the barrier energy. This implies that typically, one would have to evaluate the energy loss numerically, since this energy-dependent trajectory, except for some special cases, cannot be obtained analytically.

V. EXAMPLE – A CUBIC-POTENTIAL-LIKE MODEL

To get a better feeling for the instanton-based turnover theory, we will study a model system whereby almost everything can be performed analytically. We consider a cubic potential

$$V(q) = -\frac{M\omega^{\ddagger 2}}{2}q^2\left(1+\frac{q}{q_0}\right)+\frac{2M\omega^{\ddagger 2}q_0^2}{27} \tag{5.1}$$

with Ohmic friction $\gamma(t) = 2\gamma\delta(t)$, with γ the friction coefficient and $\delta(t)$ the Dirac δ function. From previous work [10] we know that as long as the (reduced) friction coefficient $\gamma/\omega^{\ddagger}$ is of the order of unity and lower, the PGH reduced energy loss as given in Eq. (2.8) is very close to the Mel'nikov-Meshkov energy loss. So, to simplify, we will assume that the energy loss is given by the MM form, which is

$$\delta(E) = \beta\gamma\sigma(E), \tag{5.2}$$

where $\sigma(E)$ is the real action of a trajectory moving in the well at energies between 0 and $V^{\ddagger}$. For the tunneling action we base ourselves on the vibrational perturbation theory result [32,33] as discussed in the second Appendix. Due to the symmetry of the cubic potential, we may similarly approximate the energy-dependent energy loss following MM so that

$$S(E) = \frac{4\pi V^{\ddagger}}{\lambda^{\ddagger}}\left[\frac{18}{5}\left(1-\sqrt{\frac{13}{18}+\frac{5}{18}\left(\frac{E-E_0}{V^{\ddagger}}\right)}\right)+\left(1-\frac{1}{\sqrt{1-\frac{5}{18}\frac{E_0}{V^{\ddagger}}}}\right)\left(1-\sqrt{\frac{E}{V^{\ddagger}}}\right)\right] \tag{5.3}$$

with

$$E_0 = -\frac{7\hbar^2\lambda^{\ddagger 2}}{32\times 27\times V^{\ddagger}}. \tag{5.4}$$

This form is not the exact action for a cubic oscillator but has the property that at the barrier energy $S(0) \simeq \frac{36V^{\ddagger}}{5\lambda^{\ddagger}} \times 0.94$, which is quite close to the exact action of $\frac{36V^{\ddagger}}{5\lambda^{\ddagger}}$ and $S(V^{\ddagger}) \simeq 0$ (note that for the parameters we will use, $-E_0/V^{\ddagger}$ is typically much smaller than unity).

At the same time the period associated with this action is

$$\tau = \frac{2\pi}{\lambda^{\ddagger}}\left[\frac{1}{\sqrt{\frac{13}{18}+\frac{5}{18}\left(\frac{E}{V^{\ddagger}}+\frac{7\hbar^2\lambda^{\ddagger 2}}{32\times 27\times V^{\ddagger 2}}\right)}}+\left(1-\frac{1}{\sqrt{1-\frac{5}{18}\frac{E_0}{V^{\ddagger}}}}\right)\sqrt{\frac{V^{\ddagger}}{E}}\right] \tag{5.5}$$

so that $\tau(V^{\ddagger}) \simeq 2\pi/\lambda^{\ddagger}$, that is, around the barrier energy we regain the parabolic barrier period while $\tau(0) \to \infty$ as it should. We are thus assured that this choice of an analytic form mimics semiquantitatively the true instanton action of the cubic potential.

Since the real and upside-down cubic potential lead to the same action, we use this same form to approximate the real action for motion in the well, that is, we choose

$$\sigma(E) = \frac{4\pi V^{\ddagger}}{\lambda^{\ddagger}}\left[\frac{18}{5}\left(1-\sqrt{\frac{13}{18}+\frac{5}{18}\frac{V^{\ddagger}-E}{V^{\ddagger}}}\right)\right]. \tag{5.6}$$

For this real action we have that $\sigma(0) = 0$ while $\sigma(V^{\ddagger}) \simeq \frac{36V^{\ddagger}}{5\lambda^{\ddagger}} \times 0.94$, mimicking the true action and period reasonably well. With these preliminaries we can compute the rate.

A. The spatial diffusion rate

First we compare between the "uniform Wolynes factor" of Eq. (3.13) and the parabolic-barrier-based Wolynes factor

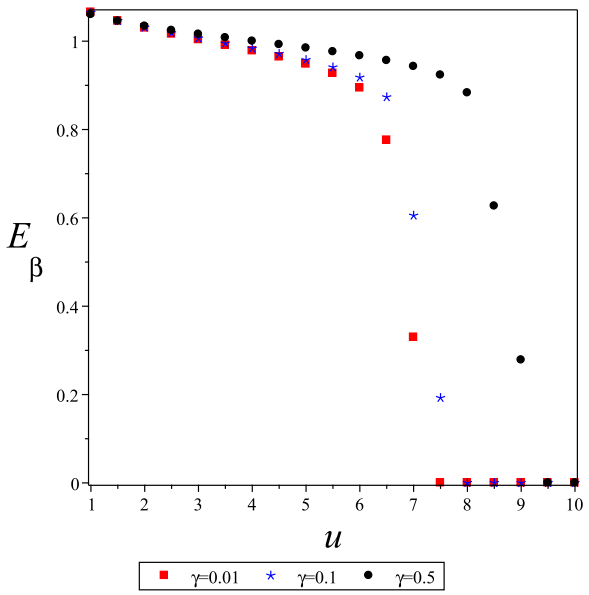

FIG. 1. The (dimensionless) steepest descent energy ($E_\beta \equiv E/V^\ddagger$) is plotted as a function of the (reduced) inverse temperature ($u = \hbar\beta\omega^\ddagger$) for a few values of the (reduced) friction coefficient $\gamma/\omega^\ddagger$.

of Eq. (2.16). For the cubic potential the well and barrier frequencies are identical in magnitude, so that the Wolynes factor depends only on the reduced inverse temperature $\hbar\beta\omega^\ddagger$ and the reduced friction coefficient $\gamma/\omega^\ddagger$. For the uniform factor one needs to estimate the thermal transmission coefficient $\kappa(\beta)$ as in Eq. (3.4). For this purpose we use the semiclassical uniform-energy-dependent transmission factor given in Eq. (3.7) and the action function given in Eq. (5.3) and perform the thermal averaging numerically. Here, we need one more parameter—the reduced barrier height $V^\ddagger/(\hbar\omega^\ddagger)$, which we take to be 4 as also used in Fig. 3 of Ref. [10], so as to facilitate the comparison with the previous results. Qualitatively, the results will be the same as long as the barrier height is larger than $\sim 5k_BT$.

The semiclassical transmission factor does not vanish at energy 0; this is one of the drawbacks of the uniform semiclassical expression. The tunneling action at this energy, even though it may be large, is finite. This implies that although the theory overcomes the divergence associated with the crossover temperature, care must be taken when considering very low temperature. When the reduced friction coefficient is not too large, and this is the region in which the depopulation factor differs from unity, one may estimate the ground-state energy in the well to be $\sim\hbar\omega^\ddagger/2$. This implies that the reduced instanton energy ($E_\beta/V^\ddagger$) should not be lower than this energy, so that with our choice of parameters, the (reduced) instanton energy should be greater than 1/8. This puts a lower limit on the temperatures to be considered.

In Fig. 1 we plot the reduced steepest descent energy ($E_\beta/V^\ddagger$) as a function of the reduced inverse temperature $u = \hbar\beta\omega^\ddagger$ for three different values of the reduced friction coefficient $\gamma/\omega^\ddagger = 0.01, 0.1$, and 0.5 using the action as given in Eq. (5.3). One notes that when the temperature is high (u small) the frictional effect is not large. However, at lower temperature the effect is marked. The stronger the friction the lower the magnitude of the normal-mode barrier frequency $\lambda^\ddagger$ [Eq. (2.5)] as compared with the bare barrier frequency $\omega^\ddagger$ [Eq. (2.3)], so that the inverse temperature at which the parabolic barrier tunneling factor diverges occurs at larger values of $\hbar\beta = \frac{2\pi}{\lambda^\ddagger} > \frac{2\pi}{\omega^\ddagger}$, and at the same time the steepest descent energy at a given value of u is higher. Increasing the friction makes the dynamics more classical-like and the steepest descent energy is then closer to the barrier height. Considering the value of $E_\beta/V^\ddagger \simeq 1/8$ as a cutoff for the largest value of u, it is also clear that this value depends on the magnitude of the friction coefficient. The dependence of the steepest descent energy on the inverse temperature shown in Fig. 1 is "generic." At high temperature the energy is close to the barrier top, and at low temperature it goes to the energy of the well bottom. Such a structure may also be seen in Fig. 1 of Ref. [24].

With this in mind we proceed to study the Wolynes factors. In Figs. 2 and 3 we plot the uniform (solid line) and the "regular" (dashed line) Wolynes factors as functions of the reduced inverse temperature for $\gamma/\omega^\ddagger = 0.1$ and 0.5, respectively. From both figures one notes that as long as $u = \hbar\beta\omega^\ddagger$ is sufficiently distant from the divergence point of the Wolynes factor, the uniform Wolynes factor is practically identical to the Wolynes factor. As one comes close to the divergence point, the Wolynes factor becomes larger than the uniform factor. The reason for this is that the parabolic barrier version of $\kappa(\beta)$ becomes too large. One also notes that as the friction increases, the divergence point moves to higher values of u, and this, too, is well understood. Increasing the friction coefficient decreases the normal-mode barrier frequency $\lambda^\ddagger$. All this has practical implications. Fitting the Wolynes factor to experimental data could lead to rather high estimates for the friction as compared to using the uniform Wolynes factor, which is a better approximation.

B. The depopulation factor

It is of interest to compare the uniform depopulation factor as given in Eq. (4.8) with the "old" parabolic-barrier-based depopulation factor as given in Eq. (4.9). In Figs. 4 and 5 we compare the uniform depopulation factor (blue solid line) with the parabolic-barrier-based factor (green, dashed line) for a reduced friction value of 0.01 and 0.05, respectively. In principle, the depopulation factor is limited to be below unity (black solid line in the left panels). This is the case for the uniform depopulation factor, but as can be seen, when u becomes sufficiently large, the parabolic-barrier-based expression becomes invalid due to the fact that $\hbar\beta\lambda^\ddagger$ becomes greater than 2π.

The low values (0.01,0.05) of the reduced friction coefficient were chosen, since at higher values the energy loss becomes too large, and the depopulation factor approaches unity for the whole temperature range considered. In both figures the right panel shows the same data as the left panel, but at a reduced range of u to show that the differences between the two depopulation factors are rather small, as long as the parabolic-barrier-based expression is valid. One notes that as the friction increases, the

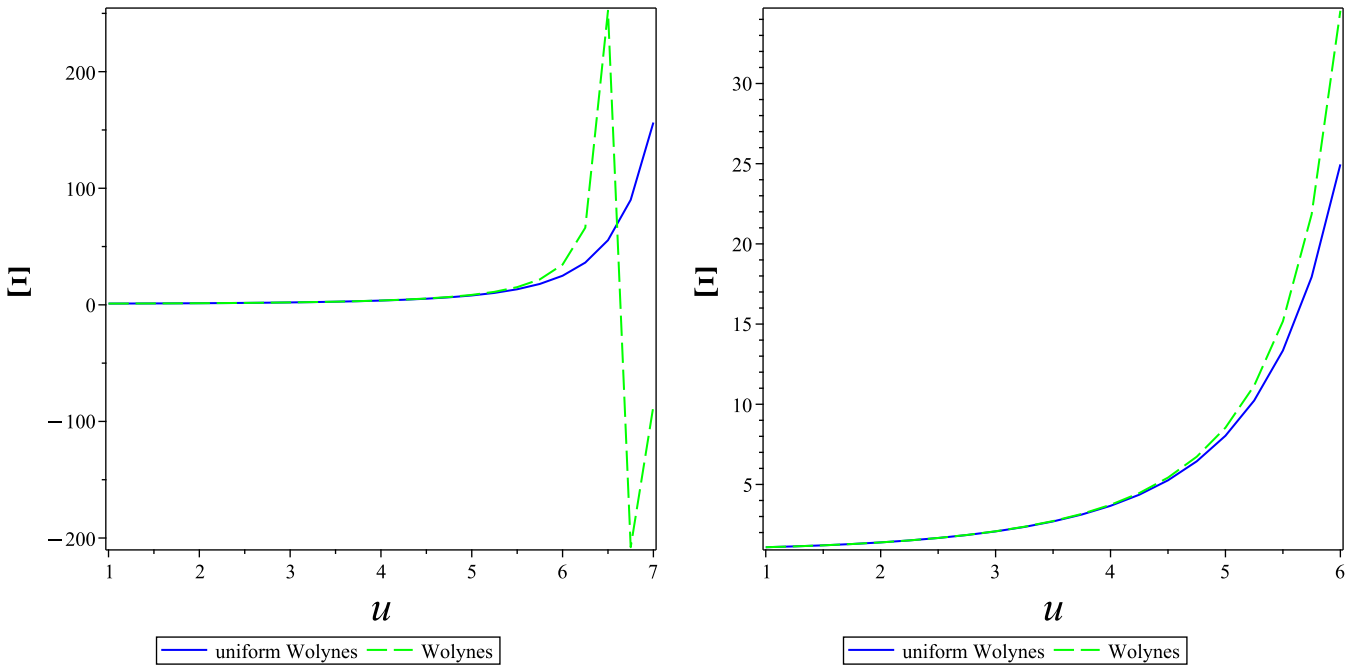

FIG. 2. Wolynes factors at a reduced friction of 0.1. $u = \hbar\beta\omega^{\ddagger}$ is the reduced inverse temperature. The green dashed line shows the Wolynes factor, the solid blue line is the uniform Wolynes factor. The left panel demonstrates the divergence of the Wolynes factor and the continuity without any divergence of the uniform Wolynes factor. The right panel shows the same data but on an expanded u scale so that the differences between the two factors at temperatures below the so-called crossover temperature are obviated. (Note that the Wolynes factors are dimensionless.)

oscillations in the parabolic barrier depopulation factor become smaller. For the model parameters we used, these oscillations become negligible when the reduced friction reaches ∼0.1; however, the expression remains invalid, as discussed.

It is also of interest to note that when the temperature is sufficiently low, even though the friction coefficient is small, the depopulation factor is close to unity. This implies that at low temperature one will hardly see the Kramers' turnover. This is discussed further in the next section.

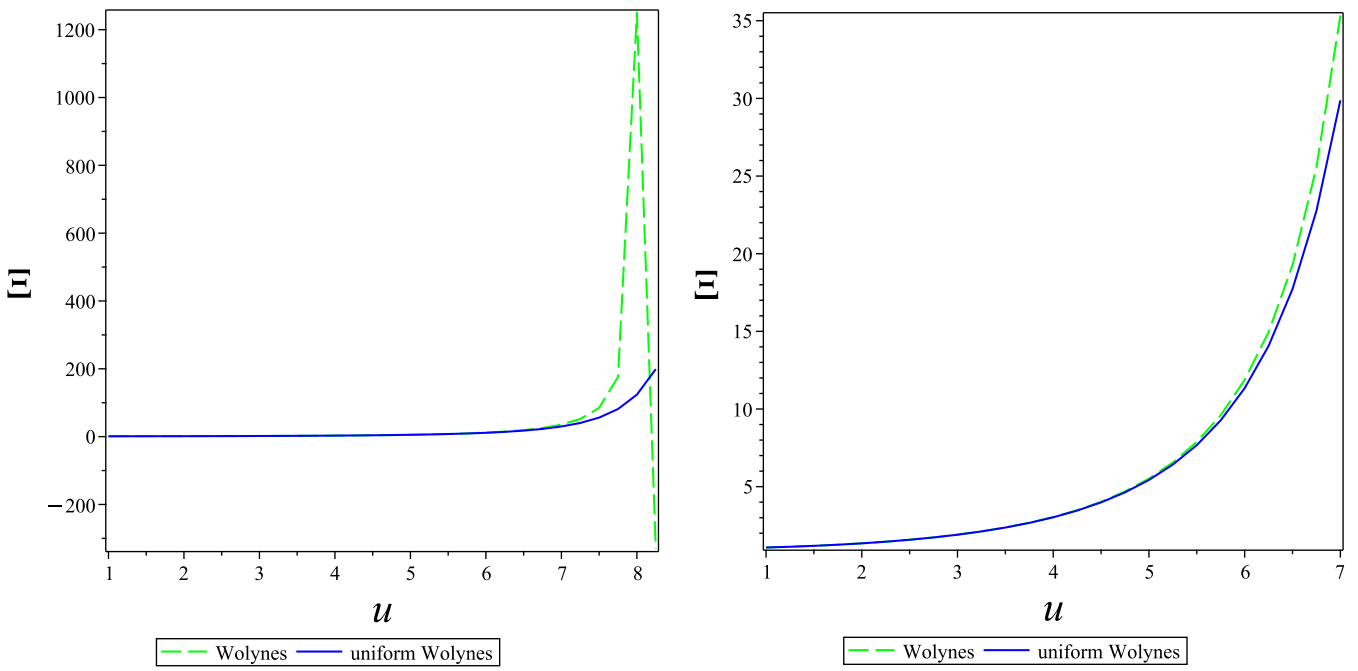

FIG. 3. Wolynes factors at a reduced friction of 0.5. Other notation is as in Fig. 2.

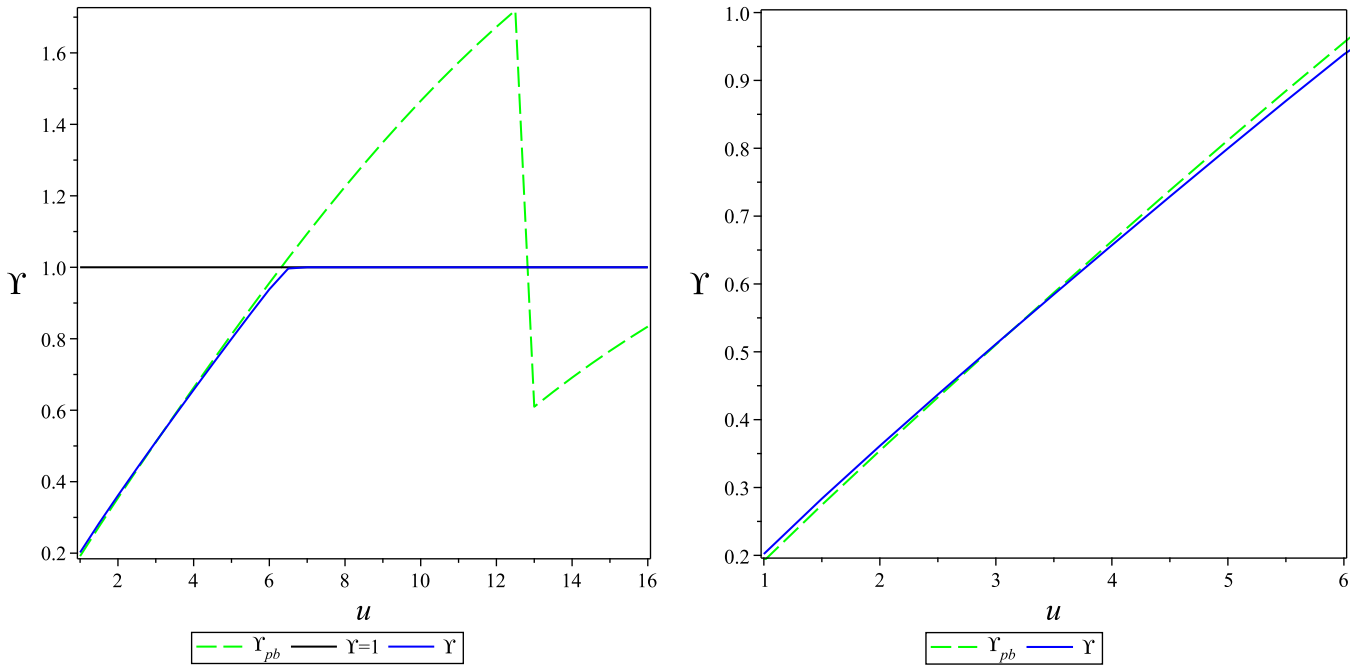

FIG. 4. Inverse temperature dependence of the (dimensionless) depopulation factors at a reduced friction of 0.01. The solid blue line shows the uniform depopulation factor, while the dashed green line shows the parabolic-barrier-based factor. The solid black line in the right panel is plotted to accentuate the value of unity. The left panel shows the dependence over a large range vs inverse temperatures to demonstrate the unphysical characteristics of the parabolic-barrier-based factor below the "crossover temperature." The right panels show that as long as $u \leqslant \sim 6$ the two factors are essentially the same.

C. The turnover rate

It remains to combine all the factors and study the resulting rate, as given in Eq. (4.10). In Fig. 6 we provide an Arrhenius plot of the (reduced) rate $(2\pi\Gamma/\omega^{\ddagger})$ for three different friction values. The results shown in the figure are qualitatively similar to the numerically exact results obtained for a similar problem by Topaler and Makri [34], and plotted in their Fig. 12. When the reduced friction is low (solid blue line), the rate shifts from a linear dependence on the inverse reduced temperature u to a flat dependence below the "crossover temperature" of $\sim 2\pi$.

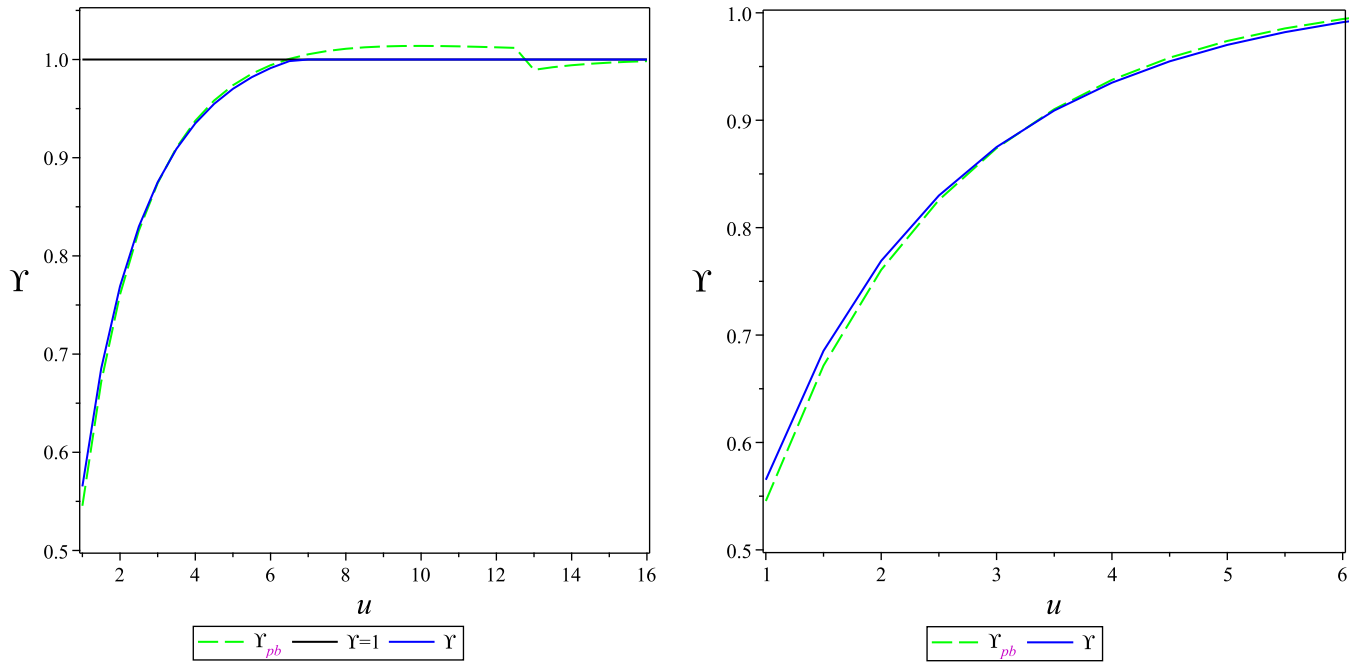

FIG. 5. Inverse temperature dependence of the depopulation factors at a reduced friction of 0.05. Other notation is as in Fig. 4.

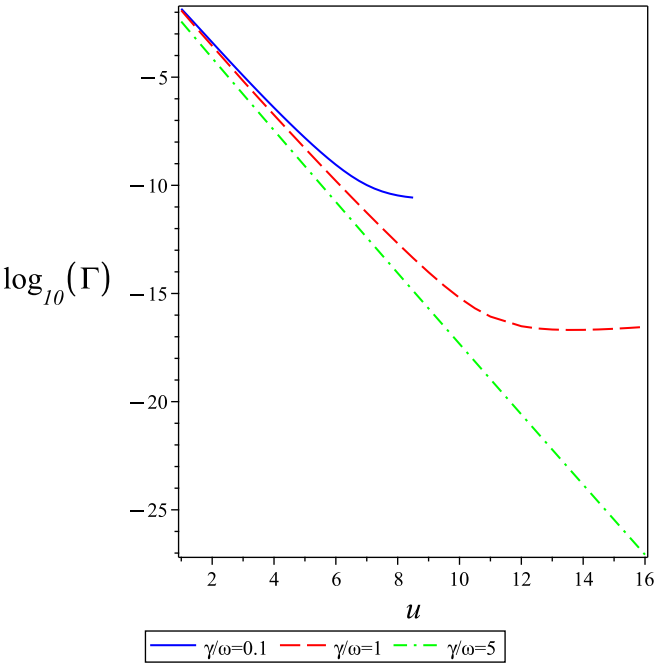

FIG. 6. Arrhenius plot of the (reduced) turnover rate (in units of $\omega^{\ddagger}$) for three different values of the (reduced) friction coefficient. The solid blue line shows results at a reduced friction of 0.1, the dashed red line at a reduced friction of unity, and the dashed green line at a reduced friction of 5. For further details, see the text.

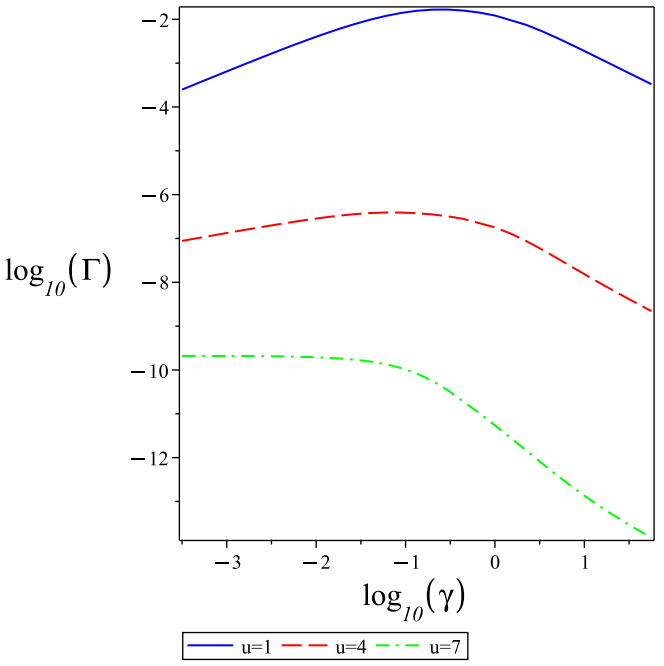

FIG. 7. Quantum-instanton-based turnover theory. The (reduced) escape rate is plotted as a function of the reduced friction coefficient for three different values of the reduced inverse temperature. The blue solid line, red dashed line, and green dashed-dotted line correspond to the inverse temperatures $u = 1, 4, 7$, respectively. The turnover is noticeable at high temperature ($u = 1$), and the turnover point moves to lower values of the friction coefficient as the temperature is reduced and finally disappears.

This is a notable result of the instanton-based turnover theory presented in this paper. For u sufficiently smaller than 2π, the previous theory [10] based on parabolic barrier transmission coefficients is valid. When u is sufficiently larger than 2π, the rate becomes temperature independent and the instanton rate is valid. The present theory reduces to both limits but importantly, also provides the expression for the rate in the region in between providing in a sense a complete theory for the quantum turnover problem. As the friction is increased, the rate decreases and tunneling sets in (as evidenced by the nonlinear dependence on u) at much lower temperature. We stress that this type of a plot would not be possible with the previous turnover theory, since it would not be valid for the low temperatures plotted here.

Finally, the central result of this section, showing the turnover, that is the actual dependence of the rate on the reduced friction coefficient at several values of the reduced temperature is plotted in Fig. 7. As already found in the numerically exact computations of Ref. [34], reducing the temperature shifts the quantum turnover point to lower friction. At low temperature, the energy loss becomes large, the depopulation factor tends to unity, and the instanton energy does not change much. When the escape is dominated by tunneling, the depopulation factor which lowers the escape rate becomes essentially irrelevant and the turnover disappears. Specifically, the data shown for $u = 7$ (green dashed-dotted line) could not be generated using the parabolic-barrier-based turnover theory.

VI. DISCUSSION

This paper presents a generalization of the quantum Kramers turnover theory whereby the divergence of the previous parabolic-barrier-based theory at the temperature $\hbar\beta\lambda^{\ddagger} = 2\pi$ is eliminated. This was achieved on the basis of the following assumptions:

(1) The theory as presented here is based on the assumption that $\beta V^{\ddagger} \gg 1$. This may be relaxed by including finite barrier corrections [27]; however, the resulting expressions do become rather involved.

(2) The original theory for the depopulation factor using parabolic barrier transmission and reflection probabilities [10], as well as the improved theory presented in this paper, are based on a perturbation theory where the small parameter is u_1^2 as defined in Eq. (2.8), which is small in the weak friction limit.

(3) The theory in the spatial-diffusion-limited regime, that is, the generalization of the Wolynes theory, is presented using a decoupling of the motion of the unstable normal mode from the stable ones. This is not necessary, one may generalize, as discussed in Ref. [25].

(4) The energy-dependent reflection and transmission coefficients are given by the uniform semiclassical expression rather than the parabolic barrier result.

(5) At a given temperature, the tunneling energy E_β is determined semiclassically through the steepest descent solution for the thermal transmission coefficient.

(6) For a given temperature the energy loss of the particle as it traverses the well is determined by the periodic trajectory across the well at the steepest descent energy E_β.

(7) Resonance phenomena in the well are ignored.

These assumptions deserve further discussion. In the previous theory, the motion of the unstable mode was naturally decoupled from the stable modes, since the theory only considered the parabolic barrier vicinity, which by definition is separable when performing the normal-mode transformation. In the spatial-diffusion-limited regime, this assumption is not essential and may be eliminated by using the multidimensional instanton theory as described in Ref. [25]. In the regime where the depopulation factor is important, necessarily, the coupling of the unstable mode to the stable modes is weak, and the decoupling approximation is reasonable.

The uniform semiclassical approximation for the rate is not perfect, but as shown on tests for the symmetric and asymmetric Eckart potentials [24] is quite reasonable, typically leading to thermal transmission coefficients which are within 10% of the exact answer, covering a very large temperature range. It is certainly more accurate than the parabolic barrier approximation and is the key to doing away with the divergence. The steepest descent approximation indicates that the central energy at which the tunneling occurs is a function of the temperature, so it is only natural to consider the dynamics around the temperature-dependent tunneling energy. In the previous theory, the energy loss was always assumed to be the energy loss at the barrier energy. At that high energy, one did not have to be as concerned with quantum resonances in the well, which certainly occur when the coupling between modes is weak. The assumption was that any resonance lifetime would be sufficiently short such that a continuum of energies would be a reasonable approximation. This assumption becomes less valid as the temperature is lowered and the transmission probability through the barrier becomes small. From this point of view, one should not consider the present theory to be very good at very low temperatures. This is, of course, true also with regards to the assumption that the unstable mode motion may be considered classically when considering the energy loss to the bath. It is these observations which are the severest criticism of the theory and indicate that it should be applied carefully at very low temperatures.

ACKNOWLEDGMENTS

I thank Prof. Peter Hänggi for his careful reading of a first draft of this paper and his insightful comments. This work was generously funded by the Israel Science Foundation (Grant No. 408/19).

APPENDIX A: DERIVATION OF EQ. (4.8)

The purpose of this Appendix is to detail the derivation of the uniform depopulation factor given in Eq. (4.8). The steps follow those given in the Appendix of Ref. [10]. Our starting point is the Laplace transformed steady-state equation (4.7):

$$\tilde{N}\left[i\left(s-\frac{\tau(\varepsilon_\beta)}{\hbar\beta}\right)\right] = -\exp\left[\frac{1}{\hbar}S(\varepsilon_\beta)+\frac{\tau(\varepsilon_\beta)\varepsilon_\beta}{\hbar\beta}\right][1-\tilde{P}(is)]\tilde{N}(is). \tag{A1}$$

One rewrites $\tilde{N}(is)$ as a product of two functions,

$$\tilde{N}(is)=\tilde{N}_1(is)\tilde{N}_2(is), \tag{A2}$$

demanding that

$$\tilde{N}_1\left[i\left(s-\frac{\tau(E_\beta)}{\hbar\beta}\right)\right] = \exp\left[\frac{1}{\hbar}S(\varepsilon_\beta)+\frac{\tau(E_\beta)\varepsilon_\beta}{\hbar\beta}\right][1-\tilde{P}(is)]\tilde{N}_1(is) \tag{A3}$$

$$\tilde{N}_2\left[i\left(s-\frac{\tau(E_\beta)}{\hbar\beta}\right)\right] = -\tilde{N}_2(is). \tag{A4}$$

The solution for $\tilde{N}_2(is)$ is readily seen to be

$$\tilde{N}_2(is) = -\frac{\pi\hbar\beta C}{\tau(E_\beta)\sin\left[\frac{\pi\hbar\beta(s+1)}{\tau(E_\beta)}\right]}, \tag{A5}$$

where C is a constant determined by the boundary condition that when the energy is much lower than the barrier, the distribution $n(\varepsilon)$ is the equilibrium distribution, so that

$$C=\frac{Q^\ddagger}{Q_0}\exp(-\beta V^\ddagger). \tag{A6}$$

Using the notation

$$\tilde{g}(is)=\ln\tilde{N}_1(is), \tag{A7}$$

one rewrites Eq. (A3) as

$$\tilde{g}\left[i\left(s-\frac{\tau(E_\beta)}{\hbar\beta}\right)\right]-\tilde{g}(is) = \ln[1-\tilde{P}(is)]+\frac{1}{\hbar}S(\varepsilon_\beta)+\frac{\tau(\varepsilon_\beta)\varepsilon_\beta}{\hbar\beta}\equiv\tilde{h}(is), \tag{A8}$$

and this has the solution

$$g(x)=\frac{h(x)}{\exp\left(\frac{\tau(\varepsilon_\beta)}{\hbar\beta}\right)-1}. \tag{A9}$$

Using the inverse Laplace transform formula, one finds (see Eq. (A11) of Ref. [10])

$$\tilde{g}(is)=\frac{\hbar\beta}{2i\tau(\varepsilon_\beta)}\int_{z-i\infty}^{z+i\infty}dy\tilde{h}(iy)\left(\cot\left[\frac{\pi\hbar\beta(s-y)}{\tau(\varepsilon_\beta)}\right]+\cot\left[\frac{\pi\hbar\beta(y+1)}{\tau(\varepsilon_\beta)}\right]\right). \tag{A10}$$

Using the definition of $\tilde{g}(is)$ [Eq. (A7)] and the relations given in Eqs. (A2) and (A5), this implies that

$$\tilde{N}(is)=-\frac{C}{\sin\left[\frac{\pi\hbar\beta(s+1)}{\tau(E_\beta)}\right]}\frac{\pi\hbar\beta}{\tau(E_\beta)}\exp\left\{\frac{\hbar\beta}{2i\tau(E_\beta)}\int_{z-i\infty}^{z+i\infty}dy\tilde{h}(iy)\left(\cot\left[\frac{\pi\hbar\beta(s-y)}{\tau(E_\beta)}\right]+\cot\left[\frac{\pi\hbar\beta(y+1)}{\tau(E_\beta)}\right]\right)\right\}. \tag{A11}$$

From the steady-state equation (4.6) we have that

$$\tilde{n}(is) = \tilde{P}(is)\tilde{N}(is). \tag{A12}$$

Using the uniform semiclassical transmission coefficient [Eq. (4.3)], noting that the escape rate is by definition

$$\Gamma = \frac{1}{2\pi\hbar\beta}\int_{-\infty}^{\infty} d\varepsilon T_{usc}(\varepsilon)n(\varepsilon) = \frac{1}{2\pi\hbar\beta}\int_{-\infty}^{\infty} d\varepsilon \exp\left[-\frac{1}{\hbar}S(\varepsilon)\right]N(\varepsilon), \tag{A13}$$

and expanding the action linearly about $S(\varepsilon_\beta)$ as in Eq. (4.5), one readily finds that

$$\Gamma = \frac{1}{2\pi\hbar\beta}\exp\left(-\left[\frac{1}{\hbar}S(\varepsilon_\beta) + \frac{\tau(E_\beta)\varepsilon_\beta}{\hbar\beta}\right]\right)\tilde{N}\left(-i\frac{\tau(\varepsilon_\beta)}{\hbar\beta}\right). \tag{A14}$$

Inserting the expression for $\tilde{N}(is)$ [Eq. (A11)], choosing the integration contour such that $z = -1/2$, and changing variables from y to

$$v = iy + i/2, \tag{A15}$$

one finds the intermediate result

$$\begin{aligned}\Gamma = {} & \frac{C}{2\tau(E_\beta)\sin\left(\frac{\pi\hbar\beta}{\tau(E_\beta)}\right)}\exp\left(-\frac{1}{\hbar}S(\varepsilon_\beta) - \frac{\tau(E_\beta)\varepsilon_\beta}{\hbar\beta}\right) \\ & \times \exp\left\{\frac{\hbar\beta}{2\tau(\varepsilon_\beta)}\int_{-\infty}^{\infty} dv\tilde{h}\left(v-\frac{i}{2}\right)\left(\cot\left[\frac{(iv+\frac{1}{2})\pi\hbar\beta}{\tau(\varepsilon_\beta)}\right] - \cot\left[\frac{\pi\hbar\beta(iv-\frac{1}{2})}{\tau(\varepsilon_\beta)}\right]\right)\right\}.\end{aligned} \tag{A16}$$

Using the identity

$$\cot z_1 - \cot z_2 = \frac{\sin(z_2 - z_1)}{\sin z_1 \sin z_2}, \tag{A17}$$

one finds after some manipulation that

$$\cot\left[\frac{(iv+\frac{1}{2})\pi\hbar\beta}{\tau(E_\beta)}\right] - \cot\left[\frac{\pi\hbar\beta(iv-\frac{1}{2})}{\tau(E_\beta)}\right] = 2\sin\left(\frac{\pi\hbar\beta}{\tau(E_\beta)}\right)\left[\cosh\left(\frac{2\pi\hbar\beta v}{\tau(E_\beta)}\right) - \cos\left(\frac{\pi\hbar\beta}{\tau(E_\beta)}\right)\right]^{-1} \tag{A18}$$

so that

$$\int_{-\infty}^{\infty} dv\left(\cot\left[\pi\frac{(iv+\frac{1}{2})\hbar\beta}{\tau(E_\beta)}\right] - \cot\left[\frac{\pi\hbar\beta(iv-\frac{1}{2})}{\tau(E_\beta)}\right]\right) = 2\left(\frac{\tau(E_\beta)}{\hbar\beta} - 1\right). \tag{A19}$$

Using the definition of $\tilde{h}(iy)$ [Eq. (A8)] and the constant C [Eq. (A6)] we find that

$$\begin{aligned}\Gamma = {} & \frac{1}{2\pi\hbar\beta}\left(\frac{\pi\hbar\beta}{\tau(E_\beta)\sin\left(\frac{\pi\hbar\beta}{\tau(E_\beta)}\right)}\right)\frac{Q^\ddagger}{Q_0}\exp\left(-\beta V^\ddagger - \frac{\beta S(\varepsilon_\beta)}{\tau(\varepsilon_\beta)} - \varepsilon_\beta\right) \\ & \times \exp\left\{\frac{\hbar\beta}{\tau(\varepsilon_\beta)}\sin\left(\frac{\pi\hbar\beta}{\tau(E_\beta)}\right)\int_{-\infty}^{\infty} dy\frac{\ln\left[1-\tilde{P}\left(y-\frac{i}{2}\right)\right]}{\cosh\left(\frac{2\pi\hbar\beta y}{\tau(E_\beta)}\right) - \cos\left(\frac{\pi\hbar\beta}{\tau(E_\beta)}\right)}\right\}.\end{aligned} \tag{A20}$$

We also note that when using the linear expansion for the action around the energy ε_β one finds that

$$\begin{aligned}\kappa_{lin}(\beta) \equiv {} & \exp(-\beta V^\ddagger)\int_{-\beta V^\ddagger}^{\infty} d\varepsilon \exp(-\varepsilon)\frac{1}{1+\exp\left(\frac{S(\varepsilon_\beta)}{\hbar} - \frac{\tau_\beta}{\beta\hbar}(\varepsilon-\varepsilon_\beta)\right)} \\ & \to_{\beta V^\ddagger\to\infty} \exp\left[-\left(\beta V^\ddagger + \frac{\beta S(\varepsilon_\beta)}{\tau_\beta} + \varepsilon_\beta\right)\right]\frac{\pi\beta\hbar}{\tau_\beta}\frac{1}{\sin\left(\frac{\pi\beta\hbar}{\tau_\beta}\right)},\end{aligned} \tag{A21}$$

so that

$$\Gamma = \frac{1}{2\pi\hbar\beta}\kappa_{lin}(\beta)\frac{Q^\ddagger}{Q_0}\exp\left\{\frac{\hbar\beta}{\tau(\varepsilon_\beta)}\sin\left(\frac{\pi\hbar\beta}{\tau(E_\beta)}\right)\int_{-\infty}^{\infty} dy\frac{\ln\left[1-\tilde{P}\left(y-\frac{i}{2}\right)\right]}{\cosh\left(\frac{2\pi\hbar\beta y}{\tau(E_\beta)}\right) - \cos\left(\frac{\pi\hbar\beta}{\tau(E_\beta)}\right)}\right\}. \tag{A22}$$

This suggests replacing $\kappa_{lin}(\beta)$ with $\kappa_{usc}(\beta)$ so that comparing with Eq. (4.10) this identifies the depopulation factor to be as in Eq. (4.8).

APPENDIX B: DETAILS OF THE CUBIC POTENTIAL-LIKE MODEL

The thermally averaged second-order vibrational perturbation theory (VPT2) [32] for the transmission coefficient is exact in one dimension to leading order in $\hbar^2$ [35] and is therefore a convenient model for obtaining analytic expressions for the instanton action. The VPT2 action in a one-dimensional system is [36]

$$S_{VPT2}(E) = \frac{\pi\lambda^{\ddagger}}{\chi}\left[-1+\sqrt{1-\frac{4\chi}{\lambda^{\ddagger 2}}(E-V^{\ddagger}-E_0)}\right], \quad \text{(B1)}$$

with

$$\chi = \frac{1}{16\lambda^{\ddagger 2}}\left[-V_4\frac{\lambda^{\ddagger 4}}{M^2\omega^{\ddagger 4}} - \frac{5}{3\lambda^{\ddagger 2}}V_3^2\frac{\lambda^{\ddagger 6}}{M^3\omega^{\ddagger 6}}\right] \quad \text{(B2)}$$

and

$$E_0 = \frac{\hbar^2}{64\lambda^{\ddagger 2}}\left[-V_4\frac{\lambda^{\ddagger 4}}{M^2\omega^{\ddagger 4}} - \frac{7}{9\lambda^{\ddagger 2}}V_3^2\frac{\lambda^{\ddagger 6}}{M^3\omega^{\ddagger 6}}\right], \quad \text{(B3)}$$

where V_j is the jth derivative of the potential at the barrier top. For the cubic potential

$$V_3 = -\frac{3M\omega^{\ddagger 2}}{q_0}, \quad V_4 = 0, \quad \text{(B4)}$$

so that

$$\chi = -\frac{15}{16}\frac{\lambda^{\ddagger 2}}{M\omega^{\ddagger 2}q_0^2} = -\frac{5}{72}\frac{\lambda^{\ddagger 2}}{V^{\ddagger}}, \quad \text{(B5)}$$

and

$$E_0 = -\frac{7\hbar^2\lambda^{\ddagger 2}}{32\times 27\times V^{\ddagger}}. \quad \text{(B6)}$$

The explicit expression for the instanton action is therefore

$$S_{VPT2}(E) = \frac{V^{\ddagger}36}{5\lambda^{\ddagger}}2\pi\left[1-\sqrt{\frac{13}{18}+\frac{5}{18}\left(\frac{E}{V^{\ddagger}}+\frac{7\hbar^2\lambda^{\ddagger 2}}{32\times 27\times V^{\ddagger 2}}\right)}\right]. \quad \text{(B7)}$$

At threshold

$$S_{VPT2}(0) = \frac{V^{\ddagger}36}{5\lambda^{\ddagger}}2\pi\left[1-\sqrt{\frac{13}{18}-\frac{5}{18}\frac{E_0}{V^{\ddagger}}}\right] \simeq \frac{36V^{\ddagger}}{5\lambda^{\ddagger}}\times 0.94, \quad \text{(B8)}$$

so that it is a good approximation to the true action of the instanton at zero energy. However, we know that the period of the instanton at $E=0$ should diverge, while

$$\tau_{SVPT2}(E) = \frac{2\pi}{\lambda^{\ddagger}\sqrt{\frac{13}{18}+\frac{5}{18}\left(\frac{E}{V^{\ddagger}}+\frac{7\hbar^2\lambda^{\ddagger 2}}{32\times 27\times V^{\ddagger 2}}\right)}} \quad \text{(B9)}$$

does not. To compensate for this, we then add a term to the instanton action:

$$S(E) = S_{VPT2}(E) + A\left(1-\sqrt{\frac{E}{V^{\ddagger}}}\right) \quad \text{(B10)}$$

such that

$$A = \frac{4\pi V^{\ddagger}}{\lambda^{\ddagger}}\left(1-\frac{1}{\sqrt{1-\frac{5}{18}\frac{E_0}{V^{\ddagger}}}}\right), \quad \text{(B11)}$$

and this assures that

$$\tau\left(V^{\ddagger}\right) = \frac{2\pi}{\lambda^{\ddagger}}, \quad \text{(B12)}$$

and on the other hand, $\tau(0)$ diverges as $1/\sqrt{E}$ when $E\to 0$. Note that $A \ll 1$ so that also

$$S(0) \simeq \frac{36V^{\ddagger}}{5\lambda^{\ddagger}}\times 0.94. \quad \text{(B13)}$$

[1] H. A. Kramers, Physica **7**, 284 (1940).
[2] V. I. Mel'nikov and S. V. Meshkov, J. Chem. Phys. **85**, 1018 (1986).
[3] E. Pollak, J. Chem. Phys. **85**, 865 (1986).
[4] E. Pollak, P. Hänggi, and H. Grabert, J. Chem. Phys. **91**, 4073 (1989).
[5] P. Hänggi, P. Talkner, and M. Borkovec, Rev. Mod. Phys. **62**, 251 (1990).
[6] R. Ianconescu and E. Pollak, Faraday Discuss. **195**, 111 (2016).
[7] R. Ianconescu and E. Pollak, J. Chem. Phys. **151**, 024703 (2019).
[8] L. Rondin, J. Gieseler, F. Ricci, R. Quidant, C. Dellago, and L. Novotny, Nat. Nanotechnol. **12**, 1130 (2017).
[9] E. Pollak and S. Miret-Artés, ChemPhysChem **24**, e202300272 (2023).
[10] I. Rips and E. Pollak, Phys. Rev. A **41**, 5366 (1990).
[11] V. I. Mel'nikov, Phys. Rep. **209**, 1 (1991).
[12] P. G. Wolynes, Phys. Rev. Lett. **47**, 968 (1981).
[13] W. H. Miller, J. Chem. Phys. **62**, 1899 (1975).
[14] S. Coleman, Phys. Rev. D **15**, 2929 (1977).
[15] J. Ankerhold, *Quantum Tunneling in Complex Systems: The Semiclassical Approach*, Springer Tracts in Modern Physics Vol. 224 (Springer, Berlin, Heidelberg, 2007).
[16] U. Weiss, *Quantum Dissipative Systems*, 5th ed. (World Scientific Publishing Co., Singapore, 2021).
[17] I. Affleck, Phys. Rev. Lett. **46**, 388 (1981).
[18] P. Hänggi and W. Hontscha, J. Chem. Phys. **88**, 4094 (1988).
[19] P. Hänggi and W. Hontcsha, Ber. Bunsenges. Phys. Chem. **95**, 379 (1991).
[20] J. Cao and G. Voth, J. Chem. Phys. **105**, 6856 (1996).
[21] M. Kryvohuz, J. Chem. Phys. **134**, 114103 (2011).
[22] Y. Zhang, J. B. Rommel, M. Y. Cvitaš, and S. C. Althorpe, Phys. Chem. Chem. Phys. **16**, 24292 (2014).

[23] S. McConnell and J. Kästner, J. Comput. Chem. **40**, 866 (2019).
[24] S. Upadhyayula and E. Pollak, J. Phys. Chem. Lett. **14**, 9892 (2023).
[25] E. Pollak, J. Chem. Phys. **159**, 224107 (2023).
[26] E. C. Kemble, Phys. Rev. **48**, 549 (1935).
[27] E. Pollak and R. Ianconescu, J. Phys. Chem. A **120**, 3155 (2016).
[28] J. L. Liao and E. Pollak, Chem. Phys. **268**, 295 (2001).
[29] R. F. Grote and J. T. Hynes, J. Chem. Phys. **73**, 2715 (1980).
[30] P. Hanggi and F. Mojtabai, Phys. Rev. A **26**, 1168 (1982).
[31] E. Pollak, Chem. Phys. Lett. **127**, 178 (1986).
[32] W. H. Miller, R. Hernandez, N. C. Handy, D. Jayatilaka, and A. Willetts, Chem. Phys. Lett. **172**, 62 (1990).
[33] T. L. Nguyen, J. F. Stanton, and J. R. Barker, J. Phys. Chem. A **115**, 5118 (2011).
[34] M. Topaler and N. Makri, J. Chem. Phys. **101**, 7500 (1994).
[35] E. Pollak and J. Cao, J. Chem. Phys. **157**, 074109 (2022).
[36] J. Stanton, J. Phys. Chem. Lett. **7**, 2708 (2016).